Nanotechnology **20** (2009) 455104 (7pp) doi:10.1088/0957-4484/20/45/455104

Gold and silver nanoparticles conjugated with heparin derivative possess anti-angiogenesis properties

Melissa M Kemp[1], Ashavani Kumar[2], Shaymaa Mousa[3], Evgeny Dyskin[3], Murat Yalcin[3], Pulickel Ajayan[2], Robert J Linhardt[1,4,5] and Shaker A Mousa[3,6]

[1] Department of Biology, Rensselaer Polytechnic Institute, Troy, NY 12180, USA
[2] Department of Mechanical Engineering and Materials Science, Rice University, Houston, TX 77005, USA
[3] The Pharmaceutical Research Institute, Albany College of Pharmacy and Health Sciences, Albany, NY 12208, USA
[4] Department of Chemistry and Chemical Biology, Rensselaer Polytechnic Institute, Troy, NY 12180, USA
[5] Department of Chemical and Biological Engineering, Rensselaer Polytechnic Institute, Troy, NY 12180, USA

E-mail: Shaker.mousa@acphs.edu

Received 3 May 2009, in final form 2 September 2009
Published 13 October 2009
Online at stacks.iop.org/Nano/20/455104

Abstract

Silver and gold nanoparticles display unique physical and biological properties that have been extensively studied for biological and medical applications. Typically, gold and silver nanoparticles are prepared by chemical reductants that utilize excess toxic reactants, which need to be removed for biological purposes. We utilized a clean method involving a single synthetic step to prepare metal nanoparticles for evaluating potential effects on angiogenesis modulation. These nanoparticles were prepared by reducing silver nitrate and gold chloride with diaminopyridinyl (DAP)-derivatized heparin (HP) polysaccharides. Both gold and silver nanoparticles reduced with DAPHP exhibited effective inhibition of basic fibroblast growth factor (FGF-2)-induced angiogenesis, with an enhanced anti-angiogenesis efficacy with the conjugation to DAPHP ($P < 0.01$) as compared to glucose conjugation. These results suggest that DAPHP-reduced silver nanoparticles and gold nanoparticles have potential in pathological angiogenesis accelerated disorders such as cancer and inflammatory diseases.

1. Introduction

Angiogenesis is the growth of new blood capillaries, and is vital to the growth and development of tissues and organs, as well as in reproduction and the repair of damaged tissues [1–3]. The process of angiogenesis is a complex process and involves many different events to occur. Various components of this process are necessary to promote new vessel formation in health and diseases. Vascular endothelial growth factor (VEGF) and fibroblast growth factor-2 (FGF-2) are important promoters of this process [4]. Both of these pro-angiogenesis growth factors bind to cell surface receptors inducing secretions of proteases and plasminogen activators, which are able to degrade the basement membrane. This degradation allows cells to migrate and proliferate at the cleared-away area and differentiate into lumen-containing vessels [4]. Several factors influence and control the growth of new vessels; however, overstimulation by such factors can cause pathological angiogenesis, promoting malignancy, inflammation and other infectious and immune disorders [1–3]. The inhibition of angiogenesis has been studied as a potential treatment for cancers by eliminating their oxygen and nourishment supply, preventing further growth and metastasis [1–3]. Many angiogenesis inhibitors have

[6] Address for correspondence: The Pharmaceutical Research Institute, Albany College of Pharmacy, One Discovery Drive, Rensselaer, NY 12144, USA.

been discovered for potential treatment in various pathological angiogenesis-mediated disorders: one of which, heparin, was identified earlier by Folkman *et al* [5] and more recently, gold nanoparticles (AuNPs) [6].

Metal nanoparticles have been important in the diverse areas of chemistry, physics and biology because of their unique optical, electrical and photothermal properties [7–12]. Metal nanoparticles have been used in probes in mass spectroscopy [13] and colorimetric detection for proteins and DNA molecules [14]. Furthermore, AuNPs have photothermal properties that can be exploited for localized heating resulting in drug release, thus increasing their potential for therapeutic applications [15]. The ease of synthesizing metallic nanoparticles and their affinity for binding many biological molecules make them attractive candidates for study. Various methods have been reported over the last two decades for the synthesis and of Au and Ag nanoparticles, which involve the reduction of metal salts with a chemical reducing agent, such as citrate acid, borohydride or other organic compounds [12–20]. The functionalization of metallic nanoparticles synthesized using such reductants is straightforward, resulting in their derivatization with biomolecules, including DNA [21] and proteins [22]. Other reducing agents have been reported to synthesize nanoparticles using biomolecules in a green methodology, such as glycosaminoglycans (GAGs) [16–18].

GAGs are negatively charged polysaccharides composed of repeating disaccharides units. These include HP, heparan sulfate, chondroitin sulfate, hyaluronan, dermatan sulfate and keratan sulfate. These GAGs, with the exception of hyaluronan, are often found attached to various core proteins, forming larger macromolecules, called proteoglycans. They are ubiquitously found throughout the body and have diverse biological functions depending on both the core protein and the type and number of GAG chains that are attached. Many of these vital functions are carried out through recognition by specific proteins of the GAG chains that are attached to the protein core. HP and heparan sulfate, for example, interact with over 100 proteins involved in anticoagulation, angiogenesis, cellular proliferation, differentiation and morphogenesis [19–21]. There is conflicting evidence for the effects of heparin on angiogenesis, whether it is pro- or anti-angiogenesis [22]. These differences in biological function are most likely due to the variations of sequence structure within the heparin chain. Fareed *et al* demonstrated that different batches and products of low molecular weight heparin had different physical and chemical compositions, leading to different biological activities [23].

Carbohydrates have been incorporated into nanomaterials as both reducing agents and stabilizing agents. The therapeutic potential of the metal nanoparticles and the biologically friendly GAGs have been extensively studied separately. However, the area of glyco-nanoparticles is just recently being investigated. The use of carbohydrates as reducing agents has been largely limited to nanoparticle synthesis, and biological activity of these composites has not been extensively explored. Previously, we demonstrated the synthesis of stable AuNPs and AgNPs using HP derivatized with a DAP group that showed effective anticoagulant activity [24]. Given the anti-angiogenesis activity of AuNPs, and the conflicting pro- and anti-angiogenesis properties of heparin, we were interested in investigating potential synergistic activities of these two agents. The current study demonstrates the feasibility of synthesizing stable GAG–nanoparticle bioconjugates to investigate effects on angiogenesis modulation by AuNPs and AgNPs. These were synthesized using HP functionalized with a DAP group as the reducing and stabilizing agent. These nanoparticles were easily purified from unbound or free heparin molecules by centrifugation and anti-angiogenesis efficacies were evaluated using a chick chorioallantoic membrane (CAM) model [25–28] and the mouse matrigel model [29–31]. *In vivo* and *in vitro* studies in various angiogenesis models used showed that the HP metal nanocomposites display potent anti-angiogenesis properties.

2. Materials and methods

2.1. Materials

Gold (III) chloride trihydrate, silver nitrate, heparinase I (E.C. 4.2.2.7) from *Flavobacterium heparinum* and Dowex-1 strongly basic anion exchange resin were purchased from Sigma Chemicals (St Louis, MO) and used as received. Heparin sodium from porcine intestinal mucosa was purchased from Celsus Laboratories (Cincinnati, OH). Other common reagents were ordered from Sigma Chemicals (St Louis, MO).

2.2. Synthesis of 2,6-diaminopyridinyl heparin (DAPHP)

The 2,6-diaminopyridinyl heparin (DAPHP) [32] was synthesized by dissolving heparin (100 mg, 8.3 μM) in 1 ml of formamide by heating at 50 °C; 2,6-diaminopyridine (100 mg, 920 μM) was then added and the reaction was maintained at 50 °C for 6 h. Aqueous sodium cyanoborohydride (9.5 mg, 150 μM) was added and incubated at 50 °C for an additional 24 h. The reaction mixture was diluted with 10 ml of water and dialyzed against 2 l of water for 48 h using a 1000 molecular weight cutoff (MWCO) dialysis membrane. The retentate was recovered, lyophilized and purified by methanol precipitation and strong anion exchange (SAX) chromatography on Dowex-1 resin.

2.3. Synthesis of gold and silver nanoparticles capped with DAPHP

Typically, an aqueous solution of $HAuCl_4$ or $AgNO_3$ (0.1 mM) was heated until boiling. DAPHP (0.5 mM aqueous solution) was added dropwise to $HAuCl_4$ or $AgNO_3$ solutions heated to boiling for 20 min. The DAPHP reduction of $HAuCl_4$ to AuNPs and $AgNO_3$ to AgNPs could be monitored by observing the change of color from a light yellow to a dark purple or yellow, respectively. The nanocomposites could be used without further purification. Alternatively, the mixture could be purified by recovering the Au-DAPHP and the Ag-DAPHP nanoparticles by centrifugation at 16 000*g* for 20 min and washed with water three times. The Au-DAPHP and Ag-DAPHP were autoclaved to sterilize these particles at 120 °C for 20 min.

2.4. Synthesis of gold and silver nanoparticles with glucose

An aqueous solution of 0.1 M of glucose was heated and stirred until boiling. A solution of $HAuCl_4$ was added dropwise to the glucose for a final concentration of 0.15 mM. The formation of particles was monitored by the change of color from light yellow to pink. Ag nanoparticles were made by boiling a solution of 0.1 M glucose and adding an aqueous solution of $AgNO_3$ for a final concentration of 0.3 mM $AgNO_3$. The solutions of Au and Ag nanoparticles were concentrated by rotary evaporation as much as possible while avoiding aggregation. The solutions were sterilized by filtering through a 0.22 μm syringe filter.

2.5. Quantification of DAPHP immobilized on gold and silver nanoparticles

DAPHP-capped Au and Ag nanoparticles were taken for analysis to determine the amount of DAPHP loading. Heparinase I (∼0.5 U in 50 mM Na_2HPO_4, 100 mM NaCl, pH 7.1) was allowed to react with 25 μl of purified Au-DAPHP and Ag-DAPHP overnight at 37 °C; the resulting solution was centrifuged (16 000*g*) to completely pelletize the nanoparticles and the heparin present in the supernatant was determined by carbazole assay [33]. Carbazole assay is a colorimetric assay used for quantification of the uronic acids present in polysaccharides.

2.6. Characterization of gold and silver nanoparticles

Ultraviolet–visible (UV–vis) and transmission electron microscopy (TEM) were used to characterize the nanocomposites. UV–vis spectroscopic measurements of the particles relied on a Perkin Elmer Lambda 950 spectrometer operated with a resolution of 2 nm. TEM was used to determine the size distribution of the particles on a Philips CM12 TEM.

2.7. Angiogenesis models

2.7.1. Chick chorioallantoic membrane assay (CAM). Ten-day-old chick embryos were purchased from SPAFAS (Preston, CT) and were incubated at 37 °C with 55% relative humidity. Chick CAM assays were performed as previously described [25–28]. A hypodermic needle was used to make a small hole in the blunt end of the egg shell, with a second hole then made on the broad side of the egg over an avascular portion of the embryonic membrane. Mild suction was applied to the first hole to displace the air sac so that the CAM dropped away from the shell. Using a Dremel drill (Racine, WI) a 1.0 cm^2 window was cut in the shell over the false air sac, allowing access to the CAM. Sterile discs of no. 1 Whatman filter paper, pretreated with 3 mg ml^{-1} cortisone acetate and PBS or FGF-2, were air dried under sterile conditions. Au or Ag nanoparticles and respective controls were applied to the chick membrane at 1.0 μg/CAM. After incubation for 3 d, each CAM beneath the filter disc was separated from the disc and rinsed with PBS. Each membrane was placed in a 35 mm Petri dish and examined under an SV6 stereomicroscope at 50× magnification. Digital images were captured and analyzed with Image-Pro software (Media Cybernetics, Silver Spring, MD). The number of vessel branch points contained in a circular region described by the filter disc was counted. One image in each CAM preparation was examined, and results from 8–10 CAM preparations were analyzed for each treatment condition.

2.7.2. Mouse matrigel model of angiogenesis. Mouse matrigel plug assay was performed in accordance with institutional guidelines for animal safety and welfare, as previously described by our laboratory [29–31]. Male mice (C57BL/6NCr) 6–8 weeks of age and weighing ∼20 g were allowed to acclimate for 5 days prior to the start of treatment. Matrigel was subcutaneously injected (three injections were made for each animal) at 100 μl/animal. Animals in the negative control group were injected with matrigel (100 μl), and animals in the positive control group were subcutaneously injected with 0.1 μg FGF-2/100 μl matrigel. Animals in the AuNPs, AgNPs or respective control groups were subcutaneously injected with 0.1 μg FGF-2 + 10 μg Au-DAPHP, Ag-DAPHP or the respective control in 100 μl of matrigel. Each group had five mice, with a total of three matrigel implants per mice subcutaneously injected. At day 12 post-plug implant all animals were sacrificed and hemoglobin contents were quantitated using a spectrophotometer assay, as previously reported [29–31].

3. Results and discussion

Synthesizing Au and Ag nanoparticles with GAGs has been previously described [24]. These metallic nanoparticles exhibited excellent stability at physiological salt concentrations. Single polydisperse nanoparticles with an average size of 10–25 nm exhibited anticoagulant and anti-inflammatory activities. Here we investigated the anti-angiogenesis properties of these nanoparticles.

The Au and Ag nanoparticles were prepared by reducing $HAuCl_4$ and $AgNO_3$ with HP. The stability of the nanoparticles is due to the interaction between the amine on the DAP moiety. Amines are able to bind to Au and Ag strongly, which can control the size and morphology of the particles [34, 35]. The formation of Au and Ag nanoparticles with the DAPHP was confirmed by analyzing the solutions by UV–vis spectroscopy. The UV–vis spectra of Au and Ag nanoparticle solutions synthesized using DAPHP are shown in figure 1. A strong resonance at approximately 525 and 410 nm, respectively, was observed for Au and Ag nanoparticles in solution, due to the excitation of surface plasmon vibrations. The color of the solutions was also a typical dark pink and yellow for Au-DAPHP and Ag-DAPHP, respectively. Nanoparticles were stabilized by the bound DAPHP and showed no aggregation. The solutions of Au-DAPHP and Ag-DAPHP were dropped onto a carbon-coated copper grid and allowed to evaporate, then analyzed by TEM. As seen in figures 2(A) and (B), TEM analysis revealed the size and shape of the Au and Ag nanoparticles, respectively. Based on these images the Au-DAPHP had a more uniform and monodisperse size and shape,

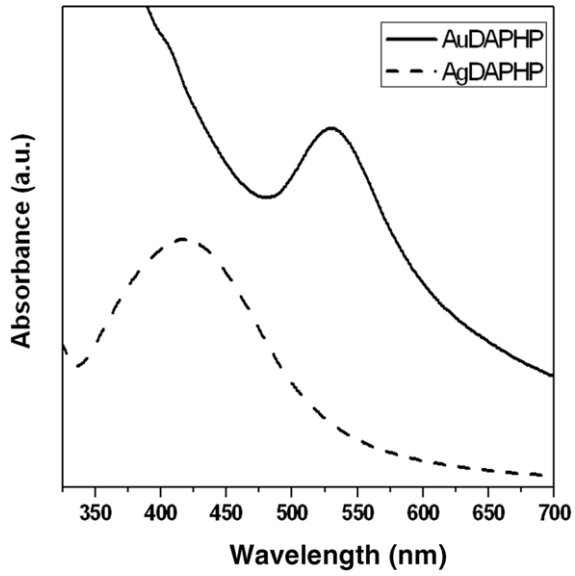

Figure 1. UV–visible spectra of gold (solid) and silver (dashed) nanoparticles synthesized by DAPHP molecules. The plasmon peak at ∼525 nm confirms the presence of AuNPs, while the plasmon peak at ∼410 nm corresponds to the formation of AgNPs. Absorbance units (a.u.).

with a majority of the particles at 14 nm ± 4 nm. The Ag-DAPHP was more polydisperse in shape and had a wider size distribution, with the majority of the particles ranging from 10 to 30 nm. This could be explained by the tighter binding between the Au surface and amine on the DAPHP, which can control the size and shape of the particles, while the Ag and the amine interactions are weaker, allowing for larger and more polydisperse particles to be formed.

Quantification of DAPHP chains bound to the surface of the purified Au-DAPHP and Ag-DAPHP nanoparticles was then determined chemically using a carbazole assay [33]. The DAPHP chains were digested off the surface of the particle, then the nanoparticles and the digested heparin fragments were separated by centrifugation to pelletize the nanoparticles. The supernatant was removed and analyzed by carbazole assay, which is a colorimetric assay that detects the uronic acids of heparin and can be analyzed spectroscopically at 525 nm. The amount of DAPHP attached to the particles was compared with free DAPHP in subsequent angiogenesis studies.

The composites, including Ag-DAPHP, Au-DAPHP, Ag-glucose, Au-glucose, HP and DAPHP at 1.0 μg DAPHP/CAM were examined for their anti-angiogenesis efficacy in inhibiting FGF-2-induced angiogenesis in the CAM model. In the CAM model, either Ag or Au nanoparticles demonstrated significant inhibition of FGF-2-induced angiogenesis as compared to the control (figures 3(A) and (B)). Au-DAPHP or Ag-DAPHP exhibited greater anti-angiogenesis efficacy ($P < 0.01$) as compared to HP, DAPHP, Ag-glucose or Au-glucose (figure 3(B)). In this regard, Au-DAPHP and Ag-DAPHP exhibited effective and comparable inhibition of FGF-2-induced angiogenesis at 83% and 76% inhibition, respectively (figure 3(B)). Heparin, DAHP, Au-glucose or Ag-glucose demonstrated significant inhibition of FGF-mediated angiogenesis (figures 4(A) and (B)) but greater inhibition was achieved with Au-DAPHP or Ag-DAPHP (figure 3(B)). Figure 4 provides illustrations of FGF-2-induced angiogenesis as compared to PBS (control) and its effective inhibition by Au-DAPHP and Ag-DAPHP nanoparticles. In agreement with the anti-angiogenesis efficacy shown in the CAM model, similar results were shown in the FGF-2 mouse matrigel model (figure 5). However, in the mouse matrigel model, all treatments, including HP, DAPHP, Au/Ag-DAPHP and Au/Ag-glucose demonstrated near-maximal and comparable anti-angiogenesis activity at 10 μg (figure 5). In this regard, testing these agents at lower doses might enable us to evaluate their relative anti-angiogenesis efficacy. Previous studies by Mukherjee *et al* [6] demonstrated the anti-angiogenesis properties of AuNPs, which might be due to the ability of AuNPs to bind to the binding domains of growth factors, leading to the inhibition of new vessel formation induced by growth factors such as FGF-2. The binding properties of

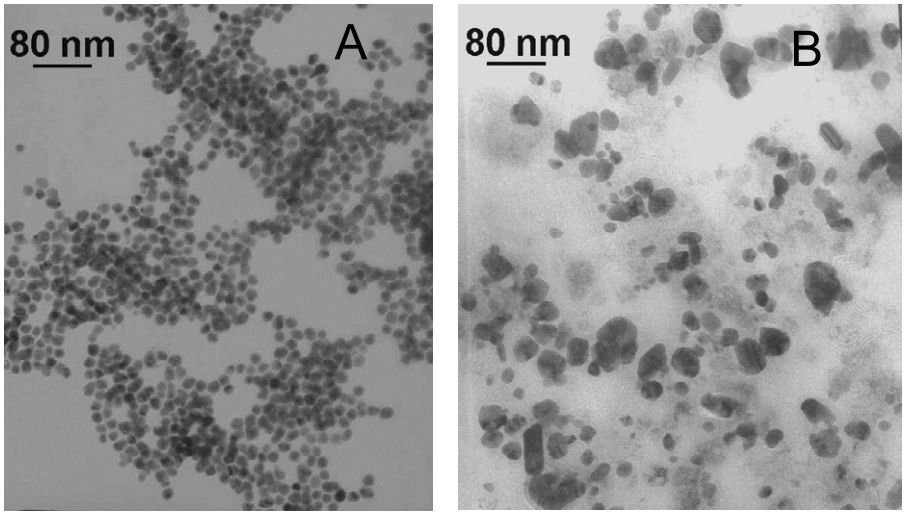

Figure 2. TEM image of (A) Au-DAPHP-capped gold nanoparticles show uniform size distribution at 125$k\times$ magnification and (B) Ag-DAPHP-capped silver nanoparticles show a more disperse size distribution at 125$k\times$ magnification.

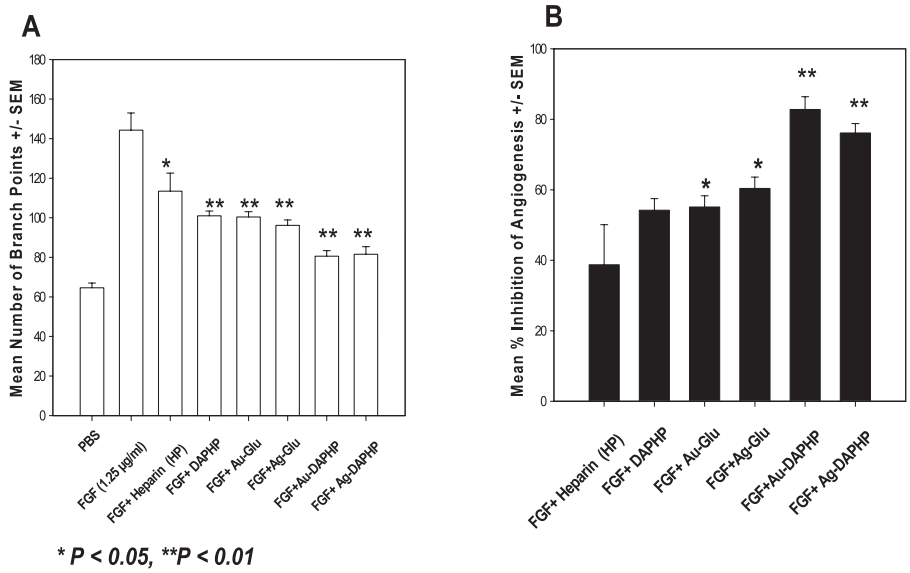

Figure 3. Effects of Au and Ag nanocomposites (1.0 μg/CAM) on FGF-2-mediated angiogenesis in the CAM model: (A) effects on mean new blood vessel branch points and (B) mean % inhibition of FGF-2-induced angiogenesis. Data represent means $\pm$SEM, $n = 8$ per group.

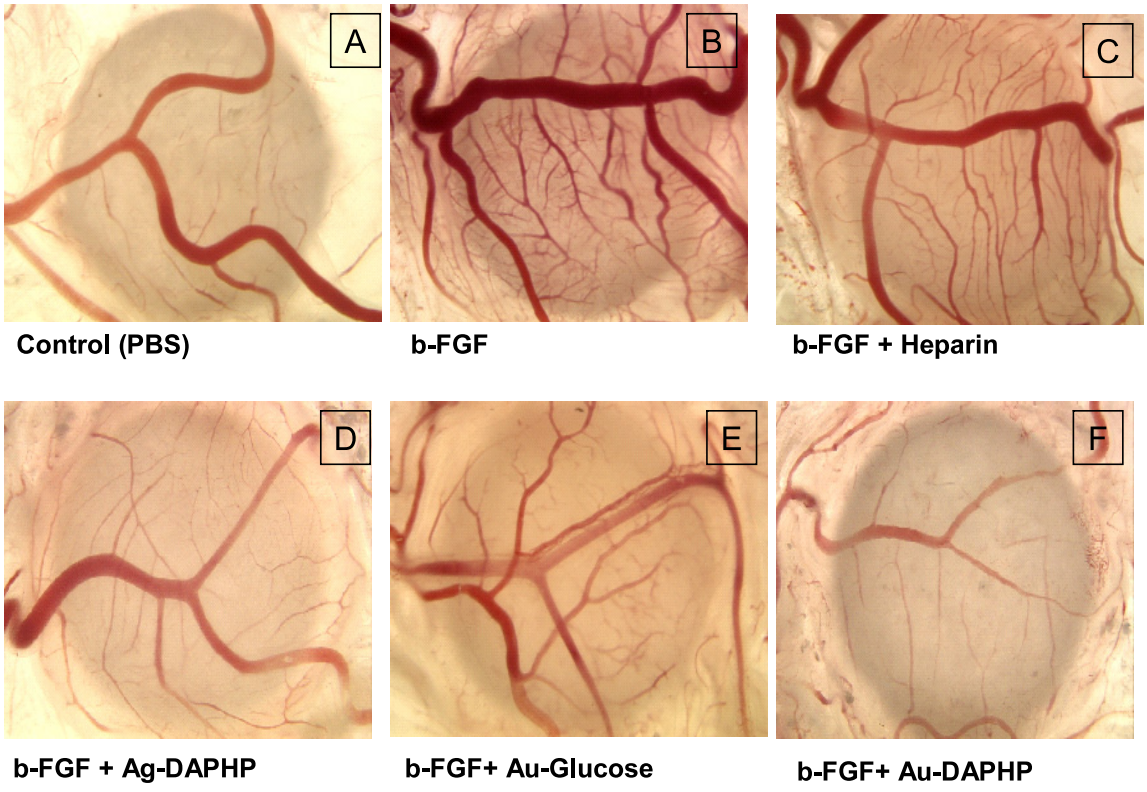

Figure 4. Representative microscopic images of angiogenesis induced in the CAM assay by (A) vehicle (PBS) control, (B) FGF2 (b-FGF), (C) b-FGF + heparin, (D) b-FGF + Ag-DAPHP, (E) b-FGF + Au-glucose and (E) b-FGF + Au-DAPHP.
(This figure is in colour only in the electronic version)

Ag are similar to that of Au, and both are able to bind to amines and thiols; therefore the explanation of the inhibitory properties of Au might also apply to that of Ag. Our results show that DAPHP conjugation to Au and Ag enhanced the anti-angiogenic effects compared with DAPHP alone and glucose-reduced Ag and Au nanoparticles in the CAM assay (figure 3(B)). HP and DAPHP exhibited limited inhibitory activity at ~39% and 54%, respectively. Earlier studies with heparin in the CAM model showed that its anti-angiogenesis efficacy might be due to its binding to FGF-2 [5]. Recent studies from our laboratory demonstrated the anti-angiogenesis efficacy of HP and its derivatives not only against FGF-2

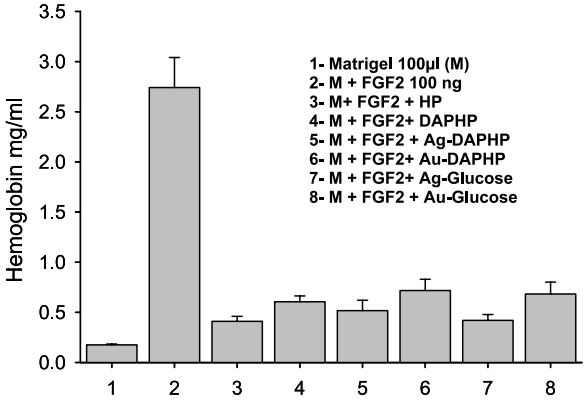

Figure 5. Effects of Au and Ag nanocomposites (10 μg/matrigel implant) on FGF2-mediated angiogenesis in the mouse matrigel model after 12 days of implant. Data represent means $\pm$SEM, $n = 15$ per group (5 mice per group $\times$ 3 plugs per animal).

but against several other growth factors including vascular endothelial growth factor (VEGF) and others [36]. The anti-angiogenesis efficacy of HP and derivatives was shown to be mainly due to the release of tissue factor pathway inhibitor (TFPI), an endogenous angiogenesis inhibitor released from endothelial cells by HP [37]. In fact, the binding of heparin to FGF-2 at low levels enhances, rather than inhibits, the pro-angiogenesis effect of the growth factor [38].

In the mouse matrigel model, either Au or Ag conjugated to glucose or DAPHP demonstrated maximal anti-angiogenesis efficacy at 10 μg DAPHP/matrigel implant (figure 5). Free Au or Ag are toxic, but glucose and HP impart biocompatibility to these particles. Conjugated Ag or Au to HP or HA showed improved anti-angiogenesis efficacy as compared to Au- or Ag-glucose. Studies from our lab with free Ag or Au metal demonstrated lethal effects (60–70% mortality at 1–10 μg/CAM) on the chick embryo but upon conjugation to form single nanoparticles, there were no lethal effects (0% mortality at 1–10 μg/CAM). Hence Ag or Au conjugation to glucose or HP improved the safety profile of these metals.

Those novel metallic nanoparticle formulations could be useful for topical applications such as psoriasis, and other dermal accelerated pathological angiogenesis.

Either Ag- or Au-conjugated DAPHP exhibited comparable anticoagulant activity to that of free HP in terms of activated partial thromboplastin time (aPTT) in human plasma, while Au- or Ag-conjugated glucose did not exhibit any anticoagulant activities (data not shown). Hence, the anti-angiogenesis efficacy of either Ag- or Au-conjugated nanoparticles is independent from the anticoagulant activity of HP since Au- or Ag-conjugated glucose exhibited significant anti-angiogenesis efficacy. Based on the anti-angiogenesis data, it appears that both Ag/Au-glucose or Ag/Au-DAPHP exhibited effective anti-angiogenesis efficacy, and having an anticoagulant along with anti-angiogenesis efficacy might be useful in some applications.

In conclusion, these nanocomposites may be useful in a wide variety of biological and biomedical applications that take advantage of the biological activities of HP and the unique physical attributes of Au and Ag core nanoparticles. The ability of DAPHP-reduced metal nanoparticles, particularly Au-DAPHP, to effectively inhibit angiogenesis shows promise for future cancer therapeutic applications. The DAPHP surrounding the particles can make these particles biologically friendly by inhibiting clotting and avoiding adverse effects linked to cancer-associated thrombosis. In conclusion, metal NPs, and in particular AuNPs, may be useful in a wide variety of biological and biomedical applications that take advantage of the intrinsic properties of HP and the unique physical attributes of Au or Ag core nanoparticles.

References

[1] Folkman J 1995 Angiogenesis in cancer, vascular, rheumatoid and other disease *Nat. Med.* **1** 27–31
[2] Carmeliet P 2005 Angiogenesis in life, disease and medicine *Nature* **438** 932–6
[3] Mousa S A 1996 Angiogenesis promoters and inhibitors: potential therapeutic implications *Mol. Med. Today* **2** 140–2
[4] Cross M J and Claesson-Welsh L 2001 FGF and VEGF function in angiogenesis: signaling pathways, biological responses and therapeutic inhibition *Trends Pharmacol. Sci.* **22** 201–7
[5] Folkman J, Weisz P B, Joullié M M, Li W W and Ewing W R 1989 Control of angiogenesis with synthetic heparin substitutes *Science* **243** 1490–3
[6] Mukherjee P, Bhattacharya R, Wang P, Wang L, Basu S, Nagy J A, Atala A, Mukhopadhyay D and Soker S 2005 Antiangiogenic properties of gold nanoparticles *Clin. Cancer Res.* **11** 3530–4
[7] Cognet L, Tardin C, Boyer D, Choquet D, Tamarat P and Lounis B 2003 Single metallic nanoparticle imaging for protein detection in cells *Proc. Natl Acad. Sci. USA* **100** 11350–5
[8] Hirsch L R, Stafford R J, Bankson J A, Sershen S R, Rivera B, Price R E, Hazle J D, Halas N J and West J L 2003 Nanoshell-mediated near-infrared thermal therapy of tumors under magnetic resonance guidance *Proc. Natl Acad. Sci. USA* **100** 13549–54
[9] Huang X, El-Sayed I H, Qian W and El-Sayed M A 2006 Cancer cell imaging and photothermal therapy in the near-infrared region by using gold nanorods *J. Am. Chem. Soc.* **128** 2115–20
[10] Li J, Wang X, Wang C, Chen B, Dai Y, Zhang R, Song M, Lv G and Fu D 2007 The enhancement effect of gold nanoparticles in drug delivery and as biomarkers of drug-resistant cancer cells *ChemMedChem* **2** 374–8
[11] O'Neal D P, Hirsch L R, Halas N J, Payne J D and West J L 2004 Photo-thermal tumor ablation in mice using near infrared-absorbing nanoparticles *Cancer Lett.* **209** 171–6
[12] Skirtach A G, Dejugnat C, Braun D, Susha A S, Rogach A L, Parak W J, Moehwald H and Sukhorukov G B 2005 The role of metal nanoparticles in remote release of encapsulated materials *Nano Lett.* **5** 1371–7
[13] Shrivas K and Wu H-F 2008 Modified silver nanoparticle as a hydrophobic affinity probe for analysis of peptides and proteins in biological samples by using liquid–liquid microextraction coupled to AP-MALDI-Ion trap and MALDI-TOF mass spectrometry *Anal. Chem.* **80** 2583–9
[14] Lee J-S, Ulmann P A, Han M S and Mirkin C A 2008 A DNA-gold nanoparticle-based colorimetric competition assay for the detection of cysteine *Nano Lett.* **8** 529–33
[15] Pissuwan D, Valenzuela S M and Cortie M B 2006 Therapeutic possibilities of plasmonically heated gold nanoparticles *Trends Biotechnol.* **24** 62–7

[16] Gole A, Kumar A, Phadtare S, Mandale A B and Sastry M 2001 Glucose induced *in situ* reduction of chloroaurate ions entrapped in a fatty amine film: formation of gold nanoparticle-lipid composites *PhysChemComm* **4** 92–5
[17] Huang H and Yang X 2004 Synthesis of polysaccharide-stabilized gold and silver nanoparticles: a green method *Carbohydr. Res.* **339** 2627–31
[18] Raveendran P, Fu J and Wallen S L 2003 Completely green synthesis and stabilization of metal nanoparticles *J. Am. Chem. Soc.* **125** 13940–1
[19] Capila I and Linhardt R J 2002 Heparin–protein interactions *Angew. Chem. Int. Edn* **41** 390–412
[20] Conrad H E 1998 *Heparin-Binding Proteins* (San Diego, CA: Academic Press) p 527
[21] Linhardt R J and Toida T 1997 Heparin oligosaccharides: new analogs development and applications *Carbohydr. Drug Des.* 277–341
[22] Mousa S A, Feng X, Xie J, Du Y, Hua Y, He H, O'Connor L and Linhardt R J 2006 Synthetic oligosaccharide stimulates and stabilizes angiogenesis: structure-function relationships and potential mechanisms *J. Cardiovasc. Pharmacol.* **48** 6–13
[23] Fareed J, Jeske W, Hoppensteadt D, Clarizio R and Walenga J M 1996 Are the available low-molecular-weight heparin preparations the same? *Sem. Thromb. Hemost.* **22** 77–91
[24] Kemp M M, Kumar A, Mousa SS, Park T-J, Ajayan P, Kubotera N, Mousa S A and Linhardt R J 2009 Synthesis of gold and silver nanoparticles stabilized with glycosaminoglycans having distinctive biological activities *Biomacromolecules* **10** 589–95
[25] Davis F B, Mousa S A, O'Connor L, Mohamed S, Lin H Y, Cao H J and Davis P J 2004 Proangiogenic action of thyroid hormone is fibroblast growth factor-dependent and is initiated at the cell surface *Circ. Res.* **94** 1500–6
[26] Ausprunk D H, Knighton D R and Folkman J 1975 Vascularization of normal and neoplastic tissues grafted to the chick chorioallantois. Role of host and preexisting graft blood vessels *Am. J. Pathol.* **79** 597–628
[27] Mousa S A, O'Connor L J, Davis F B and Davis P J 2006 Proangiogenesis action of the thyroid hormone analog 3,5-diiodothyropropionic acid (DITPA) is initiated at the cell surface and is integrin mediated *Endocrinology* **147** 1602–7
[28] Mousa S A, O'Connor L, Bergh J J, Davis F B, Scanlan T S and Davis P J 2005 The proangiogenic action of thyroid hormone analogue GC-1 is initiated at an integrin *J. Cardiovasc. Pharmacol.* **46** 356–60
[29] Mousa S A *et al* 2008 Tetraiodothyroacetic acid, a small molecule integrin ligand, blocks angiogenesis induced by vascular endothelial growth factor and basic fibroblast growth factor *Angiogenesis* **11** 183–90
[30] Mousa S A, Mohamed S, Wexler E J and Kerr J S 2005 Antiangiogenesis and anticancer efficacy of TA138, a novel alpha v beta 3 antagonist *Anticancer Res.* **25** 197–206
[31] Patra C R, Bhattacharya R, Patra S, Vlahakis N E, Gabashvili A, Koltypin Y, Gedanken A, Mukherjee P and Mukhopadhyay D 2008 Proangiogenic properties of europium(III) hydroxide nanorods *Adv. Mater.* **20** 753–6
[32] Nadkarni V D, Pervin A and Linhardt R J 1994 Directional immobilization of heparin onto beaded supports *Anal. Biochem.* **222** 59–67
[33] Bitter T and Muir H M 1962 A modified uronic acid carbazole reaction *Anal. Biochem.* **4** 330–4
[34] Leff D V, Brandt L and Heath J R 1996 Synthesis and characterization of hydrophobic, organically-soluble gold nanocrystals functionalized with primary amines *Langmuir* **12** 4723–30
[35] Kumar A, Joshi H, Pasricha R, Mandale A B and Sastry M 2003 Phase transfer of silver nanoparticles from aqueous to organic solutions using fatty amine molecules *J. Colloid Interface Sci.* **264** 396–401
[36] Mousa S A and Mohamed S 2004 Anti-angiogenic mechanisms and efficacy of the low molecular weight heparin, tinzaparin: anti-cancer efficacy *Oncol. Rep.* **12** 683–8
[37] Mousa S A and Mohamed S 2004 Inhibition of endothelial cell tube formation by the low molecular weight heparin, tinzaparin, is mediated by tissue factor pathway inhibitor *Thromb. Haemost.* **92** 627–33
[38] Norrby K and Sörbo J 1992 Heparin enhances angiogenesis by a systemic mode of action *Int. J. Exp. Pathol.* **73** 147–55